Biochemistry

Article

Cite This: Biochemistry 2019, 58, 755−762

pubs.acs.org/biochemistry

Template-Directed Catalysis of a Multistep Reaction Pathway for Nonenzymatic RNA Primer Extension

Travis Walton,[†] Lydia Pazienza,[‡] and Jack W. Szostak*[,†,‡]

[†]Howard Hughes Medical Institute, Department of Molecular Biology, and Center for Computational and Integrative Biology, Massachusetts General Hospital, Boston, Massachusetts 02114, United States

[‡]Department of Chemistry and Chemical Biology, Harvard University, 12 Oxford Street, Cambridge, Massachusetts 02138, United States

Supporting Information

ABSTRACT: Before the advent of polymerase enzymes, the copying of genetic material during the origin of life may have involved the nonenzymatic polymerization of RNA monomers that are more reactive than the biological nucleoside triphosphates. Activated RNA monomers such as nucleotide 5′-phosphoro-2-aminoimidazolides spontaneously form an imidazolium-bridged dinucleotide intermediate that undergoes rapid nonenzymatic template-directed primer extension. However, it is unknown whether the intermediate can form on the template or only in solution and whether the intermediate is prone to hydrolysis when bound to the template or reacts preferentially with the primer. Here we show that an activated monomer can first bind the template and then form an imidazolium-bridged intermediate by reacting with a 2-aminoimidazole-activated downstream oligonucleotide. We have also characterized the partition of the template-bound intermediate between hydrolysis and primer extension. In the presence of the catalytic metal ion Mg^{2+}, >90% of the template-bound intermediate reacts with the adjacent primer to generate the primer extension product while less than 10% reacts with competing water. Our results indicate that an RNA template can catalyze a multistep phosphodiester bond formation pathway while minimizing hydrolysis with a specificity reminiscent of an enzyme-catalyzed reaction.

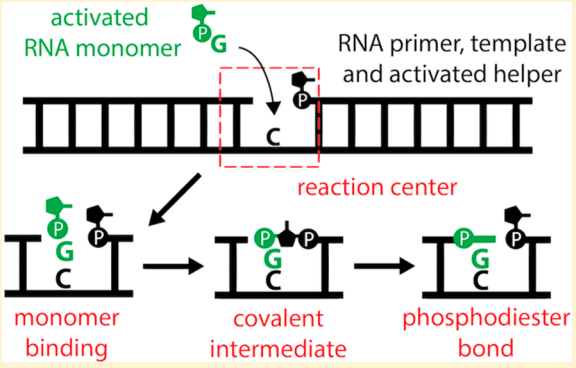

The origin of life is hypothesized to include a stage when genetic material was copied without polymerase enzymes.[1] Exactly how this might have occurred on the early Earth is unknown, but experimental models indicate that a single-stranded RNA template can direct limited polymerization of chemically activated monomers to assemble a partial complementary strand. Potentially prebiotic syntheses of activated nucleotides have recently been reported.[2,3] If complete template copying could occur, the resulting RNA duplex could then melt and each strand again behave as a template. Although this proposed cycle is simple in principle, multiple rounds of prebiotic RNA replication have not been demonstrated. Cycles of strand separation and polymerization have been demonstrated using capped DNA trimers, strand capture on magnetic beads, or enzymatic ligation of long RNA polymers,[4−6] but it is unclear if these approaches could emerge *de novo* and give rise to an evolving system. A better understanding of the nonenzymatic polymerization mechanism might identify limiting steps of the reaction pathway and offer new strategies for improving this reaction and ultimately achieving self-replication under prebiotically plausible conditions.[7]

The template-directed nonenzymatic polymerization of RNA has been extensively studied using highly activated monomers such as the nucleotide 5′-phosphoroimidazolides (^{AI}N) and the 1-hydroxy-7-azabenzotriazole esters of ribonucleotides (^{OAt}N) (Chart 1).[8,9] In recent years, nonenzymatic copying of short templates containing all four nucleotides has been achieved using activated monomers in combination with short "helper" oligomers that bind the template downstream from the site of primer extension.[10,11] Thermodynamic and structural studies indicate that helper oligonucleotides create a high-affinity single-nucleotide binding site adjacent to the primer that favors Watson−Crick hydrogen bonding over noncanonical interactions between the monomer and template.[12−14] Compared to a second downstream binding monomer, the helper oligomer also decreases the distance between the 3′-hydroxyl of the primer and the 5′-phosphate of the activated monomer, thus providing a physical explanation for their catalytic effect.[14]

Received: November 1, 2018
Revised: December 14, 2018
Published: December 19, 2018

DOI: 10.1021/acs.biochem.8b01156
Biochemistry 2019, 58, 755−762

Chart 1. Guanosine Monomers and the Dinucleotide Intermediate Used in This Study

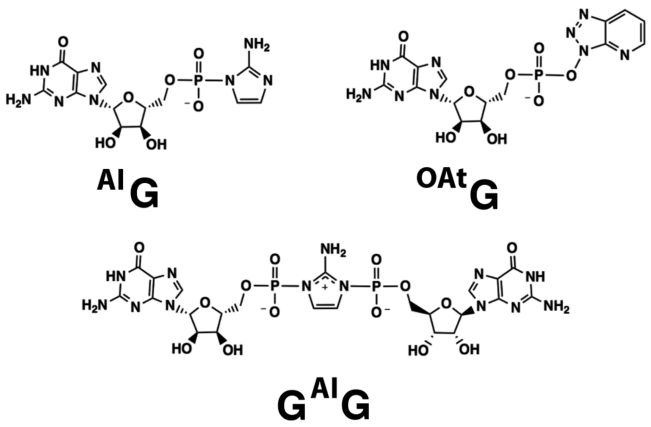

Catalysis of template-directed nonenzymatic RNA polymerization is greatly enhanced if the downstream helper oligomer is activated by 2-methylimidazole or 2-aminoimidazole on the 5′-phosphate group.[11,15] Catalysis by 2-methylimidazole- or 2-aminoimidazole-activated helper oligomers is thought to result from the formation of an imidazolium-bridged intermediate linking the 5′-phosphates of the monomer and the downstream helper. This mechanism has been previously described for nonenzymatic polymerization of imidazolide monomers,[16,17] which proceeds via the formation of an imidazolium-bridged dinucleotide intermediate ($N^{AI}N$) (Chart 1). Crystallographic studies indicate that the imidazolium-bridged intermediate is structurally preorganized to favor in-line attack by the primer 3′-hydroxyl on the adjacent phosphate of the template-bound intermediate.[18,19]

Despite the improved primer extension observed in the presence of activated downstream helpers, there are several important gaps in our understanding of the reaction. Most significantly, it is not known if the imidazolium-bridged intermediate can form on the template or only in solution.[12] Depending on the geometry of the template-bound reactants, their ability to react with each other could either be strongly inhibited or strongly accelerated. It is also unknown whether binding of an activated monomer to the template is typically followed by productive polymerization reactions or whether side reactions such as hydrolysis are more prevalent. The partition ratio between polymerization and hydrolysis is important because it would affect the long-term yield of template copying reactions.[20] For example, excessive hydrolysis of bound substrates would deplete the pool of activated monomers and disfavor polymerization.

Here, we present a mechanistic analysis of nonenzymatic RNA primer extension using RNA monomers and an activated downstream helper to determine the on-template reaction pathways. We utilize a model experimental system consisting of a primer, a helper, and a template that creates a high-affinity single-nucleotide binding site on the template between the 3′ end of the primer and the 5′ end of the helper.[12] To distinguish between template-bound reactions and off-template reactions, the activated helper (^{AI}H) is long enough to be stably bound to the template, and the primer can be extended by only one nucleotide. Our experiments show that template-bound ^{AI}G can react with an activated downstream helper to form an imidazolium-bridged intermediate ($G^{AI}H$) linking the 5′-phosphates of the monomer and the helper. This reaction is a rate-limiting step for on-template phosphodiester bond formation but can be accelerated when ^{OAt}G monomers or the $G^{AI}G$ intermediate are used in place of ^{AI}G (Chart 1). After on-template formation of the imidazolium-bridged intermediate, we observed that >90% of $G^{AI}H$ is converted to a primer extension product instead of hydrolyzing. Our results indicate that the RNA duplex on its own can specifically catalyze a multistep phosphodiester bond formation pathway over hydrolysis. This suggests that the configuration of RNA specifically favors its own replication through template-directed catalysis of polymerization.

MATERIALS AND METHODS

Materials. The free acid of guanosine 5′-monophosphate was purchased from Santa Cruz Biotechnology. 2-Aminoimidazole HCl salt was purchased from Combi-Blocks, Inc. 1-Hydroxy-7-aza-benzotriazole was purchased from Tokyo Chemical Industry Co. 2,2′-Dipyridyl disulfide was purchased from Chem-Impex International. RNA phosphoramidites were purchased from BioAutomation. The Sequagel-UreaGel concentrate and diluent system for denaturing 20% polyacrylamide gels was purchased from National Diagnostics. The 0.5 M ethylenediaminetetraacetic acid (EDTA) was purchased from Molecular Biologicals International, Inc. All other reagents were purchased from Sigma-Aldrich.

Preparation of ^{AI}G, ^{OAt}G, and $G^{AI}G$. ^{AI}G and ^{OAt}G monomers were prepared by first dissolving 100 mg of guanosine 5′-monophosphate free acid and 200 mg of either 2-aminoimidazole HCl or 1-hydroxy-7-aza-benzotriazole in ∼30 mL of water with 200 μL of triethylamine (TEA). This mixture was flash-frozen inside a polypropylene tube with liquid nitrogen and lyophilized on a VirTis Freezemobile 25EL instrument from SP Scientific. Once dry, the material was transferred to a 100 mL glass vessel with 20 mL of dimethyl sulfoxide and 300 μL of TEA. The lyophilized material did not completely dissolve at first; however, 1.5 g of 2,2′-dipyridyl disulfide (DPDS) and 1.5 g of triphenyl phosphine (TPP) were added, and the lyophilized material dissolved while the reaction mixture was left to stir at room temperature overnight. An additional 1 g of DPDS and 1 g of TPP were added the next day, and 1−2 h later, the product was precipitated by dripping into a stirring mixture of 120 mL of cold acetone, 60 mL of diethyl ether, and 4.5 g of sodium perchlorate. The crude material was collected by centrifugation in polypropylene tubes and washed two or three times with acetone. After overnight desiccation, the crude material was purified by column chromatography as previously described.[16] Fractions containing ^{AI}G were adjusted to pH 10.2−10.9 using 5% sodium hydroxide before flash-freezing and lyophilization. Fractions containing ^{OAt}G were lyophilized without pH adjustment. The $G^{AI}G$ dinucleotide was prepared as previously described.[18] Briefly, crude preparations of ^{OAt}G and ^{AI}G were mixed at high concentrations in water to form $G^{AI}G$ over 1−2 h, followed by purification via column chromatography and lyophilization at −20 °C.

Preparation of Oligomers. The sequences of all RNA oligomers used in this study are listed in Table 1. RNA sequences were either purchased from Integrated DNA Technologies, Inc., or prepared in house by standard solid-phase phosphoramidite chemistry as previously described.[21] For the preparation of the activated helper ^{AI}H, the unactivated helper was first synthesized, cleaved from the support, deprotected, and purified by C18 column chromatography.

DOI: 10.1021/acs.biochem.8b01156
Biochemistry 2019, 58, 755−762

Table 1. RNA Sequences Used in This Study

	sequence (5′ to 3′)	source
unlabeled primer	CpUpCpApApUpG	in house
labeled primer	FAM-CpUpCpApApUpG	IDT
template for G monomers	GpApGpUpUpApGpCpCpApUpUpGpApG	in house
template for C monomers	GpApGpUpUpApGpGpCpApUpUpGpApG	IDT
unactivated helper	pCpUpApApCpUpC	in house

Two micromoles of lyophilized material was then dissolved in 400 μL of dimethyl sulfoxide containing ~40 μmol of 2-aminoimidazole. Four hours after the addition of 40 mg of DPDS and TPP to begin the reaction, it was precipitated in a mixture of 10 mL of acetone, 5 mL of diethyl ether, and 0.4 g of sodium perchlorate. ^{AI}H was then purified by ion exchange chromatography and lyophilized on a VirTis Freezemobile 25EL instrument from SP Scientific without pH adjustment. pH adjustment was unnecessary to acquire pure samples, possibly due to the dilute concentration of ^{AI}H in the sample. The solid lyophilized material was washed with acetone to remove excess sodium perchlorate and placed under house vacuum overnight to remove residual acetone from the pellet. All sequences were checked for purity by liquid chromatography−mass spectrometry (LC−MS) in negative mode with an Agilent 1200 high-performance liquid chromatography (HPLC) system equipped with a Waters 100 mm XBridge C18 column connected to an Agilent 6230 mass spectrometer as previously described;[21] 50−100 pmol of material was injected for each run.

Primer Extension Reaction Kinetics. Primer extension reactions were initiated by addition of either activated nucleotides or $MgCl_2$. All reactions were performed in triplicate. If the reactions were initiated by activated nucleotides, the final concentrations in the reaction mixture were 2 μM FAM-labeled primer, 5 μM template, 250 mM NaCl, 100 mM Tris-HCl (pH 8), and 100 mM $MgCl_2$. Activated and unactivated helper oligonucleotides were added to a final concentration of 10 μM. ^{AI}G, G^{AI}G, and ^{OAt}G were added at final concentrations of 0.025−2 mM to initiate primer extension reactions. If the reactions were initiated with $MgCl_2$, a preincubation mix containing 2 μM FAM-labeled primer, 5 μM template, 10 μM ^{AI}H, 250 mM NaCl, 100 mM Tris (pH 8), and 0.025−2 mM monomer was prepared. The monomer was added last at various concentrations to initiate the preincubation period. After various times, 1 M $MgCl_2$ was added to the preincubation mix to yield a final concentration of 100 mM $MgCl_2$, which dilutes the components of the preincubation mix to 90% of their original value. Addition of $MgCl_2$ marks the beginning of the primer extension reaction. Reaction aliquots (1 μL) were removed at various times, and reactions quenched in 7 μL of 8 M urea, 100 mM Tris-HCl, 100 mM boric acid, and 75 mM EDTA. Two microliters of the quenched reaction mix was analyzed by 20% denaturing polyacrylamide gel electrophoresis (PAGE); 0.4 mM thick gels were run for 30 min at a 30 W constant power on a Bio-Rad model 3000/300 power supply. Then, the gels were scanned on an Amersham Typhoon RGB instrument from GE Healthcare and analyzed with IQTL 8.1 software to quantify the fluorescent bands.

After quantification by PAGE, data were analyzed to determine rate constants. The pseudo-first-order rate constant k_{obs} was determined by linear regression of the natural log of the fraction remaining primer over time using Microsoft Excel. Error bars are not presented if they are smaller than the data symbols used for the graph. To determine k_{bridge}, the data were fit to a standard integrated equation of consecutive first-order kinetics using Prism 7 that relates the formation of the primer extension product over time to the two first-order rate constants k_{bridge} and k_{extend}. The general consecutive first-order equation for the formation of product C from initial reactant A over time X is $[C] = [A]\{1 + [1/(k_1 - k_2)] \times [k_2 \times \exp(-k_1X) - k_1 \times \exp(-k_2X)]\}$, For calculation of the rate constant k_{bridge}, the data from the primer extension time courses were fit to the equation [extended primer] = 2×10^{-6} M $\times \{1 + [1/(k_{bridge} - 0.45\ min^{-1})] \times [0.45\ min^{-1} \times \exp(-k_{bridge}X) - k_{bridge} \times \exp(-0.45\ min^{-1} \times X)]\}$, where 2×10^{-6} M is the starting concentration of the unextended primer, X is the time in minutes, and k_{extend} = 0.45 min^{-1} = 27 h^{-1}.

Analytical High-Performance Liquid Chromatography (HPLC). Samples were analyzed on an Agilent 1100 series HPLC system equipped with a 4.6 mm × 250 mm, 6 μm Varitide RPC column, a solvent degasser, an autosampler, and a fraction collector. Samples were monitored for absorbance at a wavelength of 254 nm using a gradient of 20 mM triethyl amine/bicarbonate buffer (pH 7.5) versus acetonitrile (2% ACN from 0 to 5 min, 2 to 13% ACN (for G monomers) and 2 to 15% ACN (for C monomers) from 2 to 30 min, ≤95% ACN from 32 to 37 min, down to 2% ACN from 38 to 40 min). To monitor the formation of G^{AI}H during the preincubation of ^{OAt}G with the P/^{AI}H/T complex, 25 μL preincubation reaction mixtures were prepared with final concentrations of 20 μM primer, 22 μM template, 24 μM ^{AI}H, 40 mM Tris (pH 8), 250 mM NaCl, and 200 μM ^{OAt}G. Addition of 1 M $MgCl_2$ to a final concentration of 100 mM $MgCl_2$ in the preincubation mix, to initiate primer extension, caused the reaction volume to reach 27.8 μL, and as a result, all of the components of the preincubation mixture were diluted to 90% of their original concentration. To monitor the appearance of reaction products, 20 μL of the reaction mix was injected into the HPLC instrument for all preincubation mixes and for the samples incubated with 100 mM $MgCl_2$ for 10 min. For the samples incubated in 100 mM $MgCl_2$ for 1 and 3 min, the 27.8 μL reaction mixture was mixed with 10 μL of 0.5 M EDTA at the indicated time, and 30 μL of this reaction mixture was injected as quickly as possible into the HPLC instrument.

The elution of reactants and products from the HPLC instrument was monitored by the ultraviolet absorbance at 254 nm, and the A_{254} peak integrals were used to calculate concentrations as follows. First, a correction factor was applied to account for the different extinction coefficients of the primer versus the primer +1 product, as well as ^{AI}H and unactivated helper H versus G^{AI}H. Extinction coefficients at 260 nm were calculated using the OligoAnalyzer 3.1 software from Integrated DNA Technologies. Second, the concentrations of the primer and primer +1 were calculated using the ratio of the two integrals to normalize the total concentration to 20 μM, the initial primer concentration. The same was done for ^{AI}H, G^{AI}H, and unactivated helper H, to normalize the total concentration to 24 μM, the initial ^{AI}H concentration. Third, the concentration of GMP and ^{OAt}G was calculated from the ratio of their HPLC integrals, normalizing the total

DOI: 10.1021/acs.biochem.8b01156
Biochemistry 2019, 58, 755−762

concentration of GMP, ^{OAt}G, primer +1, and G^{AI}H to 200 μM, the initial ^{OAt}G concentration.

To collect peak fractions for subsequent MS analysis, a 20 min preincubation mix of 75 μL or a 10 min primer extension reaction mix of 83 μL was prepared, and 70 μL of the sample was injected into the HPLC instrument. Fractions corresponding to the peaks were automatically collected by an absorbance threshold. Fractions were flash-frozen in liquid nitrogen and lyophilized at −20 °C on a VirTis AdVantage Plus EL-85 lyophilizer from SP Scientific to concentrate the sample. Samples were then submitted to the LC−MS instrument as described for oligo synthesis. Experimentally observed masses were compared to the exact masses calculated using ChemDraw Professional 16.0 to calculate the differences listed in Table S1.

RESULTS AND DISCUSSION

On-Template Catalysis of Primer Extension by Downstream Helpers. We began our analysis of the on-template reactions in a primer/activated G monomer/activated helper/template (P/^{AI}G/^{AI}H/T) complex by determining whether the predominant mechanism of primer extension proceeded via on-template formation of the G^{AI}H intermediate, which has a 2-aminoimidazolium group linking the 5′-phosphates of the monomer and the helper (Scheme 1). In this proposed reaction pathway, the RNA monomer guanosine 5′-phosphoro-2-aminoimidazolide (^{AI}G) first binds the single-nucleotide gap between the primer and the helper, forms the G^{AI}H intermediate, and finally reacts with the primer to form the +1 extended primer, with regeneration of ^{AI}H. We also considered the possibility that the ^{AI}G RNA monomer could react off-template to form the dinucleotide intermediate G^{AI}G and that G^{AI}G might also extend the primer but without forming an imidazolium-bridged intermediate with the downstream activated helper ^{AI}H.

Scheme 1. Predominant On-Template Reactions of ^{AI}G and G^{AI}G To Form the Imidazolium-Bridged G^{AI}H Intermediate and Extend the Primer by One Nucleotide

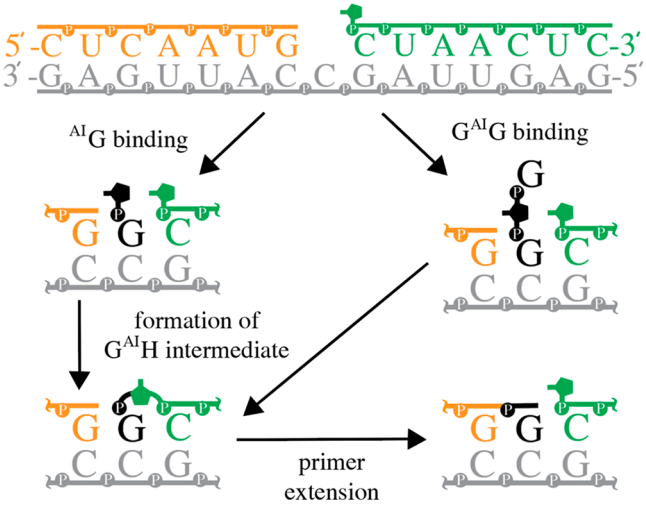

To determine whether primer extension requires the on-template formation of an imidazolium bridge between the monomer and the downstream helper, we examined primer extension reactions using the ^{AI}G monomer or the G^{AI}G intermediate, with either no downstream helper, a downstream helper with a 5′-phosphate, or a downstream helper with a 5′-phosphoro-2-aminoimidazole group (Figure 1a–c). As an additional control, we also analyzed a differently activated RNA monomer, guanosine 5′-phosphoro-(1-hydroxy-7-aza-benzotriazole) [^{OAt}G (Chart 1)], which cannot react with itself but can react with ^{AI}G to form the imidazolium-bridged dinucleotide intermediate G^{AI}G.[18,22] For ^{AI}G, G^{AI}G, and ^{OAt}G, the activated helper ^{AI}H increased the rate of primer extension by at least 50-fold and in most cases >200-fold in comparison with the rate with the unactivated helper or no helper (Table 2). The large magnitude of the rate enhancement suggests that the predominant pathway of primer extension with ^{AI}G, G^{AI}G, and ^{OAt}G involves the on-template formation of the imidazolium-bridged G^{AI}H intermediate.

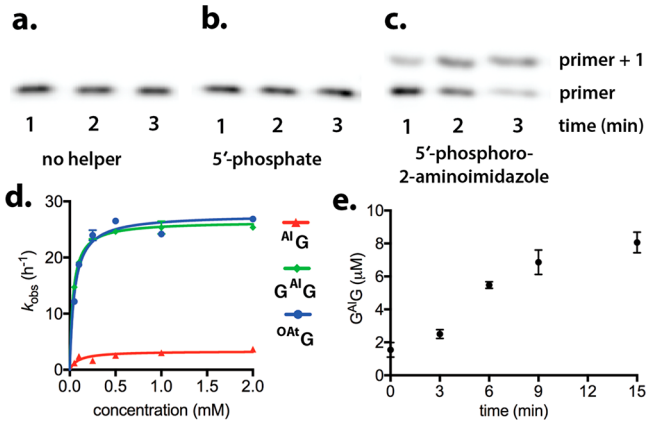

Figure 1. Imidazolium bridge formation with the downstream helper is required for fast rates of primer extension. Polyacrylamide gel electrophoresis of primer extension reactions at 1, 2, and 3 min with 2 mM ^{OAt}G and (a) no downstream helper, (b) the unactivated helper, and (c) the 2-aminoimidazole-activated helper. (d) The observed pseudo-first-order rate constant of primer extension (k_{obs}) within the P/^{AI}H/T complex increases and plateaus with the concentration of ^{AI}G, G^{AI}G, and ^{OAt}G. The line is a fit to the Michaelis−Menten equation. (e) The concentration of G^{AI}G in a solution of 500 μM ^{AI}G incubated in primer extension buffer as measured by HPLC.

The observed pseudo-first-order rate constants of primer extension, k_{obs}, are presented in units of inverse hours. Reactions were initiated by addition of 2 mM ^{AI}G, G^{AI}G, or ^{OAt}G to a reaction mix containing 2 μM primer, 5 μM template, and either no downstream helper oligonucleotide, 10 μM unactivated helper, or 10 μM activated helper oligonucleotide ^{AI}H. For reactions with no helper or unactivated helper, the reaction was quantified at 20 min, 1 h, and 3 h. For reactions with ^{AI}H, the reaction was quantified at 1, 2, and 3 min. We conservatively consider our detection limit to be $<10^{-2}$ h^{-1}, which corresponds to 3% extension over 3 h.

The slower rate of primer extension with ^{AI}G than with G^{AI}G or ^{OAt}G (Table 2) is consistent with the fact that both imidazolium species and OAt are better leaving groups than AI and that therefore both G^{AI}G and ^{OAt}G should react to form the G^{AI}H intermediate more rapidly than ^{AI}G. However, a previous study suggested that the affinity of an RNA nucleotide for the template also depends on the identity of the activating group on the 5′-phosphate of the monomer,[22] suggesting that the rate difference could potentially be due to differential binding. We therefore measured the rate of primer extension as a function of the concentration of ^{AI}G, G^{AI}G, and ^{OAt}G (Figure

DOI: 10.1021/acs.biochem.8b01156
Biochemistry 2019, 58, 755−762

Table 2. Rates of Primer Extension for ^{AI}G, G^{AI}G, and ^{OAt}G Depend on the Presence and Activation of a Downstream Helper Oligonucleotide

	^{AI}G	G^{AI}G	^{OAt}G
no helper	$<10^{-2}$	$(1.6 \pm 0.1) \times 10^{-2}$	$<10^{-2}$
unactivated helper	$(6.8 \pm 0.3) \times 10^{-2}$	$(1.1 \pm 0.0) \times 10^{-1}$	$(9.7 \pm 0.2) \times 10^{-2}$
^{AI}H	3.7 ± 0.1	25.3 ± 0.4	26.9 ± 0.4

1d). The pseudo-first-order rate constant of primer extension, k_{obs}, increased with the concentration for all three molecules and plateaued above 500 μM, suggesting saturation of the template. However, the rate of ^{AI}G plateaus at 3.7 h^{-1}, while those of G^{AI}G and ^{OAt}G plateau at 27 h^{-1}. Thus, differences in binding do not account for the differences in the rate of primer extension. Because fast primer extension requires an activated downstream helper, the most likely explanation for the observed differences in rate is that they reflect differences in the rate of formation of the G^{AI}H intermediate, which is required for primer extension.

Because of the slow rate of extension by ^{AI}G, we checked whether the spontaneous formation of G^{AI}G in the reaction mixture impacted our measurements of primer extension by ^{AI}G. Our best preparation of the ^{AI}G monomer still contained trace amounts of G^{AI}G (Figure 1e), corresponding to 1.5 ± 0.4 μM G^{AI}G in a solution of 500 μM ^{AI}G. Incubation of 500 μM ^{AI}G in primer extension buffer resulted in an additional slight increase in the concentration of G^{AI}G to 2.5 ± 0.3 μM by 3 min. However, this amount of G^{AI}G cannot account for the rate of primer extension with ^{AI}G in the presence of ^{AI}H, which was measured at time points from 1 to 3 min (Figure S1). This observation further suggests that template-bound ^{AI}G does react directly with the downstream helper ^{AI}H to form the intermediate G^{AI}H, albeit at a slow rate.

Quantifying On-Template Formation of the Imidazolium-Bridged Intermediate. In the experiments described above, the rate of primer extension is an indirect readout of the rate of formation of the G^{AI}H intermediate, and we therefore sought a more direct test of the hypothesis that the slow rate of primer extension by ^{AI}G was due to rate-limiting on-template formation of intermediate G^{AI}H. If the on-template reaction of ^{AI}H and ^{AI}G to form G^{AI}H is rate-limiting, then primer extension should become faster if the ^{AI}G is preincubated with the primer/activated helper/template (P/^{AI}H/T) complex, allowing the G^{AI}H intermediate to accumulate before initiation of the primer extension reaction. To test this hypothesis, 1 mM ^{AI}G was preincubated with the P/T/^{AI}H complex in the absence of the catalytic metal ion Mg^{2+} to allow accumulation of the G^{AI}H intermediate. After various times, 100 mM $MgCl_2$ was then added to initiate primer extension.

The k_{obs} of primer extension significantly increased after preincubation of the P/^{AI}H/T complex with ^{AI}G and plateaus near 21 h^{-1} by 30 min (Figure 2a), consistent with the accumulation of the G^{AI}H intermediate leading to faster subsequent rates of primer extension. Preincubation of 1.5 mM ^{AI}G in buffer without the P/^{AI}H/T complex did not greatly increase the rate of primer extension, indicating that the off-template formation of G^{AI}G does not account for this effect. Repeating this experiment with 1 mM ^{OAt}G instead of ^{AI}G slightly increased the k_{obs} of primer extension from 24 to 28 h^{-1}, suggesting that with ^{OAt}G, the bulk of the G^{AI}H intermediate forms very rapidly but that preincubation allows for a small further increase in G^{AI}H levels. A similar maximum k_{obs} value of ~27 h^{-1} was also observed for initial rates of

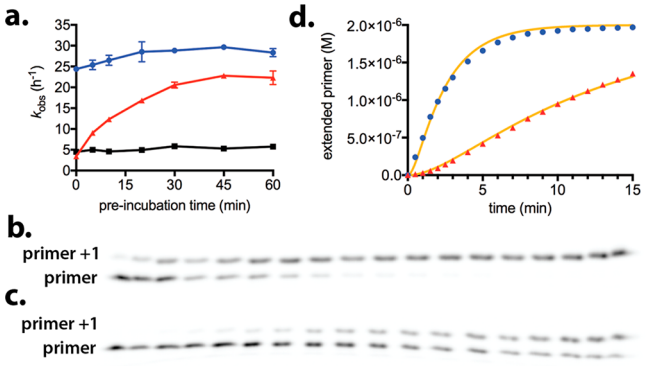

Figure 2. On-template imidazolium bridge formation between ^{AI}G and ^{AI}H limits the rate of primer extension. (a) k_{obs} of primer extension vs time of preincubation of 1 mM ^{AI}G with the P/^{AI}H/T complex (red triangles), 1 mM ^{OAt}G with the P/^{AI}H/T complex (blue circles), or 1.5 mM ^{AI}G without the P/^{AI}H/T complex (black squares). PAGE shows quick formation of the extension product for (b) ^{OAt}G vs (c) ^{AI}G. (d) Formation of the primer extension product over the first 15 min with 2 mM ^{AI}G or ^{OAt}G, fit to a model of consecutive first-order reactions (yellow lines). For panels b–d, time points are every 30 s for the first 3 min and then every minute thereafter.

primer extension at saturating levels of ^{OAt}G and G^{AI}G without preincubation (Figure 1d), suggesting that this value may correspond to the maximum rate of phosphodiester bond formation in this experimental system when ^{AI}H is completely converted to the G^{AI}H intermediate. The k_{obs} of ^{AI}G does not reach this value of 27 h^{-1}, even after preincubation, possibly due to slower formation of G^{AI}H and concomitant hydrolysis of this intermediate.

To quantify the rate of on-template imidazolium bridge formation, we performed a time course of primer extension when the P/^{AI}H/T complex was incubated with a saturating concentration (2 mM) of either ^{AI}G or ^{OAt}G.[12] After primer extension had been initiated by addition of ^{AI}G or ^{OAt}G, time points were taken to capture the reaction kinetics over 15 min (Figure 2b,c, quantification in panel d). Once the monomer binds the P/^{AI}H/T complex, primer extension occurs through two steps, imidazolium bridge formation followed by phosphodiester bond formation, that have associated rate constants k_{bridge} and k_{extend}, respectively. Both of these rate constants should be first-order because the reactions occur within a bound complex. When k_{bridge} is much greater than k_{extend}, the primer extension reaction can be approximated by a single first-order rate constant k_{extend}. This scenario likely represents the maximum rate observed at saturating levels of ^{OAt}G and G^{AI}G (Figure 1d). Therefore, we set k_{extend} to 27 h^{-1} in a simple model of consecutive first-order kinetics. This model was then fit to the primer extension time courses to calculate the rate of imidazolium bridge formation (Figure 2d). We calculated k_{bridge} values of 5.1 ± 0.03 h^{-1} for ^{AI}G and 137 ± 14 h^{-1} for ^{OAt}G. The previously determined second-order rate constant for imidazolium-bridged dinucleotide formation from

DOI: 10.1021/acs.biochem.8b01156
Biochemistry 2019, 58, 755–762

2-aminoimidazole-activated monomers free in solution is 4.5 h^{-1} M^{-1}.[17] This suggests that the effective on-template molarity is ~1.1 M. However, this value is likely an upper limit due to the possible contribution of $G^{AI}G$ formed off template during the 15 min time course.

Mg^{2+} Promotes Primer Extension over Hydrolysis. For the time course of primer extension during ^{OAt}G incubation with the P/^{AI}H/T complex, we noticed that >98% of the primer is extended by 15 min (Figure 2b). This suggests that very little of the $G^{AI}H$ hydrolyzes to a helper oligonucleotide with a 5′-phosphate (Scheme 2), because the rate of primer extension with an unactivated helper is very slow (Table 2). However, hydrolysis of the $G^{AI}H$ intermediate to guanosine 5′-monophosphate (GMP) and ^{AI}H could still occur on template without greatly affecting the rate and yield of primer extension because ^{OAt}G is in excess and could exchange with template-bound GMP. To measure the rate of this hydrolysis reaction, we prepared the P/$G^{AI}H$/T complex by *in situ* formation of $G^{AI}H$ using low concentrations of ^{OAt}G (Figure S2) and then proceeded to measure the partitioning of this complex between primer extension and hydrolysis to yield GMP. A low concentration of the monomer was necessary to limit the amount of off-template hydrolysis, so that on-template hydrolysis could be observed.

Scheme 2. High Partition of the P/$G^{AI}H$/T Complex to the Primer +1 Extension Product over Hydrolysis

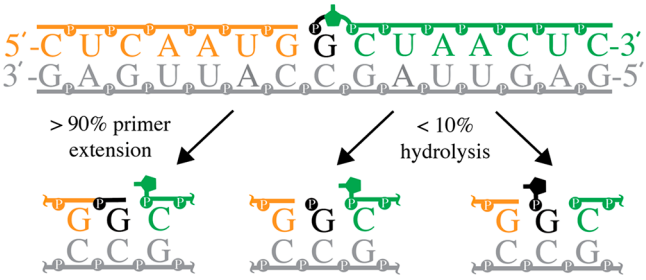

To verify the *in situ* formation of the $G^{AI}H$ intermediate using this method, we incubated the ^{OAt}G monomer with the P/^{AI}H/T complex in the absence of Mg^{2+} and analyzed the products by reverse-phase HPLC (Figure 3a). All components of the P/^{AI}H/T complex were well-resolved and identified by comparison with standards or by LC−MS analysis (Figures S3 and S4 and Table S1). Upon addition of 200 μM ^{OAt}G, a new peak appeared (Figure 3a, purple) corresponding to $G^{AI}H$. As expected, its formation requires both the template and downstream helper activation (Figure S5); in addition, the collected material from this peak has the expected mass and extends the primer with a k_{obs} of 26 ± 0.9 h^{-1} (Figure S6).

The concentration of the $G^{AI}H$ intermediate plateaus at 16 μM after a 20 min preincubation of 20 μM P/^{AI}H/T complex with 200 μM ^{OAt}G (Figure 3b), but hydrolysis and extension products slowly accumulate (Figure S7). Therefore, we analyzed the Mg^{2+}-initiated partition of $G^{AI}H$ between hydrolysis and primer extension after a 20 min preincubation. At this point, 80% of the primer is in a P/$G^{AI}H$/T complex, <5% of the primer has reacted to form the primer +1 product, and the remaining primer is present in the unreacted P/^{AI}H/T complex (Figure 3c). Addition of $MgCl_2$ caused rapid accumulation of the primer +1 product, from <1 to >18 μM, while the level of unreacted primer correspondingly decreased from 19 to 2 μM, as confirmed by LC−MS (Table S1). As

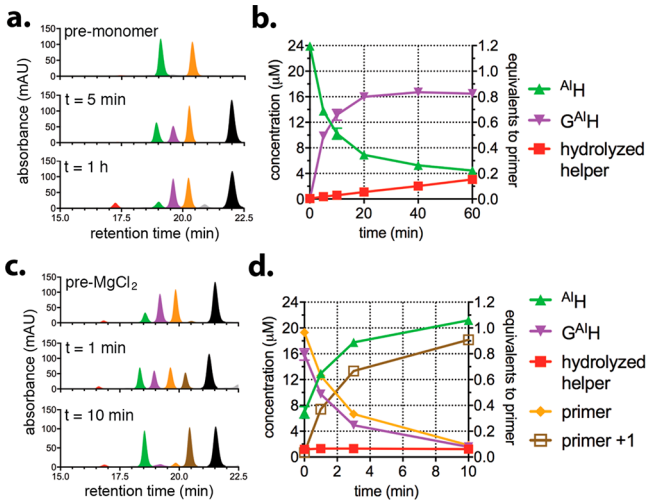

Figure 3. Imidazolium-bridged $G^{AI}H$ intermediate that undergoes phosphodiester bond formation with minimal hydrolysis. (a) Reverse-phase HPLC detects the $G^{AI}H$ formed *in situ* from ^{OAt}G and the P/^{AI}H/T complex without Mg^{2+}. (b) Quantification by HPLC shows that formation of $G^{AI}H$ plateaus near a 20 min preincubation. (c) HPLC analysis of the preincubation complex after addition of 100 mM $MgCl_2$. (d) Quantification by HPLC over time shows a high level of conversion of $G^{AI}H$ to the primer extension product and ^{AI}H. Legend: red, unactivated helper; green, ^{AI}H; purple, $G^{AI}H$; yellow, primer; brown, primer +1; black, ^{OAt}G.

expected, primer extension required both the template and activation of the downstream helper (Figure S8). By 10 min, >90% of the primer had been extended, suggesting that the $G^{AI}H$ intermediate reacts with the primer to form a new phosphodiester bond with high specificity and little accompanying hydrolysis (Scheme 2).

To quantitate the partition of the P/$G^{AI}H$/T complex between reaction of $G^{AI}H$ with the primer and hydrolysis, we calculated the changes in the concentration of the remaining reaction products of both primer extension and hydrolysis during the 10 min incubation in the presence of the catalytic metal ion Mg^{2+}. The concentration of ^{AI}H increased from 6.9 ± 0.9 to 21 ± 0.03 μM during the primer extension reaction, as expected because reaction of the primer with $G^{AI}H$ releases ^{AI}H as the leaving group. In contrast, the level of the unactivated helper (derived from attack of water on the phosphate between 2-aminoimidazole and the RNA oligonucleotide) was not observed to significantly increase. Similarly, we did not observe a significant change in the concentration of GMP, the product of attack of water on the phosphate between G and the AI of $G^{AI}H$ (Figure S9). Before the addition of $MgCl_2$, the concentration of GMP was 21 ± 0.7 μM, while after incubation with $MgCl_2$ for 10 min, the measured GMP concentration was the same within error at 20 ± 1.0 μM.

To test the generality of this result, we also examined extension of the primer using the OAt-activated C monomer ^{OAt}C in place of ^{OAt}G but with the same activated helper ^{AI}H. The template sequence was also changed to contain a G in the +1 position to maintain Watson−Crick pairing between the monomer and template. These results using ^{OAt}C are consistent with what was observed in the experimental system described above (Figure S10). After *in situ* formation of the imidazolium-bridged $C^{AI}H$ intermediate on the template, addition of Mg^{2+} caused rapid conversion to the primer

DOI: 10.1021/acs.biochem.8b01156
Biochemistry 2019, 58, 755−762

extension product and ^{AI}H without significant hydrolysis of the ^{OAt}C monomer.

CONCLUSIONS

The most effective one-pot nonenzymatic template-directed RNA polymerization reactions utilize 2-aminoimidazole-activated monomers and 2-aminoimidazole-activated downstream helper trinucleotides to copy templates containing all four nucleotides by primer extension.[15] Our current results show that when a 2-aminoimidazole-activated monomer ^{AI}N is bound to the template, it can react with an adjacent template-bound helper ^{AI}H to form an imidazolium-bridged intermediate N^{AI}H, which subsequently undergoes phosphodiester bond formation by reaction with the adjacent primer 3′-OH. However, activated downstream trimers, which can rapidly come on and off the template, might also react with ^{AI}N or N^{AI}N off template to form an imidazolium-bridged species that then binds the template and reacts with the primer. The relative contributions of these pathways to primer extension remain unknown.

From a practical perspective, the improved mechanistic understanding of the role of downstream helpers in primer extension suggests new strategies for further enhancement of the rate and extent of primer extension. For example, replacing ^{AI}G with either ^{OAt}G or G^{AI}G increased the rate of primer extension by >7-fold. In addition, the reaction of ^{AI}G with ^{AI}H to form G^{AI}H releases free 2-aminoimidazole, which inhibits primer extension.[17] This problem is mitigated if ^{OAt}G or G^{AI}G is used in place of ^{AI}G. The utilization of a more reactive monomer or dinucleotide intermediate in combination with 2-aminoimidazole-activated trimer helpers could also decrease the necessary concentrations of primer extension substrates to more prebiotically plausible levels. Typical primer extension conditions utilize 20−100 mM monomers, but by using a combination of ^{OAt}G and ^{AI}H, we were able to decrease the RNA monomer concentration to ≤200 μM while maintaining high rates of polymerization (Figure 3 and Figure S2). A lower monomer concentration should also reduce side reactions that produce inhibitors of primer extension, such as nucleotide 5′-phosphates and 5′,5′-pyrophosphate-linked dinucleotides.[23,24]

While the ultimate goal of our mechanistic studies is to enable nonenzymatic copying of any RNA template sequence, our current study focused on the addition of just a single nucleotide to a primer, by using a long, stably bound downstream helper. This approach allowed us to quantitatively follow the on-template reactions and to track potential side reactions. We initially expected that Mg^{2+}-catalyzed attack of the primer 3′-hydroxyl on the G^{AI}H intermediate (which generates a new phosphodiester bond) might also be associated with Mg^{2+}-catalyzed attack of water on the imidazolium-bridged intermediate, causing hydrolysis. The complex protein machinery required for the catalytic specificity of enzyme polymerases suggested that nonenzymatic polymerization might be relatively nonspecific. To our surprise, no significant hydrolysis reactions were detected in the presence of Mg^{2+} during the time required for primer extension (Figure 3), indicating that Mg^{2+} specifically catalyzes on-template phosphodiester bond formation instead of hydrolysis.

We propose that the structure of the transient complex generated by interaction between the Mg^{2+} ion and the site of nonenzymatic polymerization does not allow for the attack of water on the reactive imidazolium intermediate. Our recent observation of primer extension by X-ray crystallography shows that the template-bound configuration of G^{AI}G is positioned for in-line attack by the 3′-OH of the primer, but the catalytic Mg^{2+} ion was not observed.[19] One possibility is that the Mg^{2+} is transiently coordinated by both the 3′-OH of the primer and the 5′-phosphate of the reactive nucleotide. If Mg^{2+} coordination helps orient the 3′-OH for in-line attack on the phosphate, then the imidazolium-bridged intermediate would be sterically occluded from hydrolysis by either Mg^{2+}-bound water or water from the bulk solution. It will be interesting to see if the high partition of the imidazolium-bridged intermediate to primer extension products is unique to RNA or is also seen with other nucleic acids; it is possible that the selectivity of the primer extension reaction was an important reason for the selection of RNA as the genetic material during the origin of life.

ASSOCIATED CONTENT

Supporting Information

The Supporting Information is available free of charge on the ACS Publications website at DOI: 10.1021/acs.biochem.8b01156.

Figures S1−S10 and Table S1 (PDF)

AUTHOR INFORMATION

Corresponding Author

*E-mail: szostak@molbio.mgh.harvard.edu.

ORCID

Travis Walton: 0000-0001-6812-1579

Jack W. Szostak: 0000-0003-4131-1203

Funding

J.W.S. is an Investigator of the Howard Hughes Medical Institute. This work was supported in part by a grant from the National Science Foundation (CHE-1607034) to J.W.S. and a grant (290363) from the Simons Foundation to J.W.S. L.P. was supported by a National Science Foundation Graduate Research Fellowship Program (DGE1144152 and DGE1745303).

Notes

The authors declare no competing financial interest.

ACKNOWLEDGMENTS

The authors thank Chun Pong Tam and Lijun Zhou for help with oligonucleotide synthesis and purification and Victor Lelyveld for assistance with LC−MS.

ABBREVIATIONS

^{AI}G, guanosine 5′-phosphoro-2-aminoimidazolide; G^{AI}G, di-guanosine 2-aminoimidazolium-bridged intermediate; GMP, guanosine 5′-monophosphate; G^{AI}H, 2-aminoimidazolium-bridged intermediate linking the 5′-phosphates of a guanosine monomer and a helper; ^{OAt}G, guanosine 5′-phosphoro-(1-hydroxy-7-aza-benzotriazole); P/^{AI}G/^{AI}H/T complex, primer/activated G monomer/activated helper/template complex; P/^{AI}H/T complex, primer/activated helper/template complex.

REFERENCES

(1) Joyce, G. F., and Szostak, J. W. (2018) Protocells and RNA Self-Replication. *Cold Spring Harbor Perspect. Biol. 10*, a034801.

(2) Fahrenbach, A. C., Giurgiu, C., Tam, C. P., Li, L., Hongo, Y., Aono, M., and Szostak, J. W. (2017) Common and Potentially

DOI: 10.1021/acs.biochem.8b01156
Biochemistry 2019, 58, 755−762

Prebiotic Origin for Precursors of Nucleotide Synthesis and Activation. *J. Am. Chem. Soc. 139*, 8780−8783.
(3) Mariani, A., Russell, D. A., Javelle, T., and Sutherland, J. D. (2018) A Light-Releasable Potentially Prebiotic Nucleotide Activating Agent. *J. Am. Chem. Soc. 140*, 8657−8661.
(4) Sievers, D., and von Kiedrowski, G. (1994) Self-replication of complementary nucleotide-based oligomers. *Nature 369*, 221−224.
(5) Hänle, E., and Richert, C. (2018) Enzyme-Free Replication with Two or Four Bases. *Angew. Chem., Int. Ed. 57*, 8911−8915.
(6) He, C., Gállego, I., Laughlin, B., Grover, M. A., and Hud, N. V. (2017) A viscous solvent enables information transfer from gene-length nucleic acids in a model prebiotic replication cycle. *Nat. Chem. 9*, 318−324.
(7) Sosson, M., and Richert, C. (2018) Enzyme-free genetic copying of DNA and RNA sequences. *Beilstein J. Org. Chem. 14*, 603−617.
(8) Weimann, B. J., Lohrmann, R., Orgel, L. E., Schneider-Bernloehr, H., and Sulston, J. E. (1968) Template-directed synthesis with adenosine-5′-phosphorimidazolide. *Science 161*, 387.
(9) Hagenbuch, P., Kervio, E., Hochgesand, A., Plutowski, U., and Richert, C. (2005) Chemical primer extension: efficiently determining single nucleotides in DNA. *Angew. Chem., Int. Ed. 44*, 6588−6592.
(10) Deck, C., Jauker, M., and Richert, C. (2011) Efficient enzyme-free copying of all four nucleobases templated by immobilized RNA. *Nat. Chem. 3*, 603−608.
(11) Prywes, N., Blain, J. C., Del Frate, F., and Szostak, J. W. (2016) Nonenzymatic copying of RNA templates containing all four letters is catalyzed by activated oligonucleotides. *eLife 5*, e17756.
(12) Tam, C. P., Fahrenbach, A. C., Björkbom, A., Prywes, N., Izgu, E. C., and Szostak, J. W. (2017) Downstream Oligonucleotides Strongly Enhance the Affinity of GMP to RNA Primer-Template Complexes. *J. Am. Chem. Soc. 139*, 571−574.
(13) Zhang, W., Tam, C. P., Wang, J., and Szostak, J. W. (2016) Unusual Base-Pairing Interactions in Monomer-Template Complexes. *ACS Cent. Sci. 2*, 916−926.
(14) Zhang, W., Tam, C. P., Zhou, L., Oh, S. S., Wang, J., and Szostak, J. W. (2018) Structural Rationale for the Enhanced Catalysis of Nonenzymatic RNA Primer Extension by a Downstream Oligonucleotide. *J. Am. Chem. Soc. 140*, 2829−2840.
(15) Li, L., Prywes, N., Tam, C. P., O'Flaherty, D. K., Lelyveld, V. S., Izgu, E. C., Pal, A., and Szostak, J. W. (2017) Enhanced Nonenzymatic RNA Copying with 2-Aminoimidazole Activated Nucleotides. *J. Am. Chem. Soc. 139*, 1810−1813.
(16) Walton, T., and Szostak, J. W. (2016) A Highly Reactive Imidazolium-Bridged Dinucleotide Intermediate in Nonenzymatic RNA Primer Extension. *J. Am. Chem. Soc. 138*, 11996−12002.
(17) Walton, T., and Szostak, J. W. (2017) A Kinetic Model of Nonenzymatic RNA Polymerization by Cytidine-5′-phosphoro-2-aminoimidazolide. *Biochemistry 56*, 5739−5747.
(18) Zhang, W., Tam, C. P., Walton, T., Fahrenbach, A. C., Birrane, G., and Szostak, J. W. (2017) Insight into the mechanism of nonenzymatic RNA primer extension from the structure of an RNA-GpppG complex. *Proc. Natl. Acad. Sci. U. S. A. 114*, 7659−7664.
(19) Zhang, W., Walton, T., Li, L., and Szostak, J. W. (2018) Crystallographic observation of nonenzymatic RNA primer extension. *eLife 7*, e36422.
(20) Yarus, M. (2017) Efficient Heritable Gene Expression Readily Evolves in RNA Pools. *J. Mol. Evol. 84*, 236−252.
(21) Tam, C. P., Zhou, L., Fahrenbach, A. C., Zhang, W., Walton, T., and Szostak, J. W. (2018) Synthesis of a Nonhydrolyzable Nucleotide Phosphoroimidazolide Analogue That Catalyzes Nonenzymatic RNA Primer Extension. *J. Am. Chem. Soc. 140*, 783−792.
(22) Kervio, E., Sosson, M., and Richert, C. (2016) The effect of leaving groups on binding and reactivity in enzyme-free copying of DNA and RNA. *Nucleic Acids Res. 44*, 5504−5514.
(23) Puthenvedu, D., Janas, T., Majerfeld, I., Illangasekare, M., and Yarus, M. (2015) Poly(U) RNA-templated synthesis of AppA. *RNA 21*, 1818−1825.
(24) Majerfeld, I., Puthenvedu, D., and Yarus, M. (2016) Cross-backbone templating; ribodinucleotides made on poly(C). *RNA 22*, 397−407.

DOI: 10.1021/acs.biochem.8b01156
Biochemistry 2019, 58, 755−762